

Electronic Structure of $(\text{Ga}_{1-x}\text{Zn}_x)\text{N}_{1-x}\text{O}_x$ Photocatalyst for Water Splitting by Hybrid Hartree-Fock Density Functional Theory Methods

Cristiana Di Valentin

Dipartimento di Scienza dei Materiali, Università di Milano-Bicocca, via Cozzi 53, 20125 Milano, Italy

Received: November 26, 2009; Revised Manuscript Received: March 2, 2010

GaN:ZnO solid solutions have been identified as a promising system for photocatalytic or photoelectrochemical water splitting under visible-light irradiation. However, the origin of their activity at longer wavelength with respect to the parent materials (GaN and ZnO) absorbing in the UV spectrum is still matter of debate. Previous theoretical studies were based on standard GGA or GGA+U calculations which largely underestimated the band gap values of the two semiconductors and are thus not best suited methods for the required analysis. The present is a hybrid density functional study (B3LYP) which provides more accurate description of the electronic structure of the parent semiconductors and is thus also more reliable for the evaluation of the mixed GaN:ZnO system. For small concentrations of ZnO in GaN, local inhomogeneity of Zn or O concentration must be invoked to observe a red-shift of the absorption edge. For larger concentrations, some random alloy distributions, enthalpically more expensive but entropically more favorable, are found to present reduced band gap values because of a positive shift of the N 2p states from the GaN component interfacing the ZnO fragments as a consequence of the repulsive interaction with the Zn 3d states.

Introduction

Solar hydrogen production can be achieved in various ways, but photocatalytic or photoelectrochemical water splitting is one of the most attractive because it is simple and can be applied to large-scale production by means of powdered photocatalysts.¹ Since the first report of Honda–Fujishima on TiO_2 in the early 1970s,² most of the materials used for photocatalytic water splitting are oxides. However, these are UV-active materials which are commonly activated in the visible region by introduction of dopants. The doping approach has many drawbacks and limitations, such as the increased recombination rate at the dopant center.³ As well as oxides, also some nitrides are found to be active for water splitting and in particular GaN powders are active under UV irradiation.⁴ Recently, it has been shown that a nitride:oxide (GaN:ZnO) solid solution, prepared by NH_3 treatment of a mixture of Ga_2O_3 and ZnO at above 1100 K, presents excellent absorption properties in the visible region and interesting catalytic performances for hydrogen production under visible light irradiation.^{5–9} The main characteristic of the (oxy)nitride compound is that the top of the valence band edge is made up by the N 2p states and thus the photogenerated holes are free to travel in the valence band, in contrast with the localized N 2p states in N-doped oxides.^{10–13}

Given the interest on this promising solid solution, recently few theoretical papers^{14–16} have appeared in the literature, trying to provide a rationalization for the visible light activity of the mixture, given that the two starting materials (GaN and ZnO) absorb only in the UV light spectrum. These works are based on standard DFT/GGA calculations,¹⁴ and in some cases^{15,16} the DFT+U correction has been introduced to improve the description of the semicore d states of Ga and Zn. However, the computed band gap values for the two systems are rather poor, especially as far as ZnO is concerned (computed 1.6 eV versus exp. value of 3.4 eV for ZnO; 2.4 eV versus 3.5 eV for GaN). The rationalization which has been proposed for the experimental findings is that the band gap narrowing is due to p–d

repulsion between Zn 3d and N 2p states in the upper valence band. Since the underestimation of the band gaps is so severe, it is questionable whether the analysis is correct.

Moreover, it has been recently proposed, on the basis of photoluminescence (PL) and photoluminescence excitation (PLE) studies, that the origin of the visible light absorption arises from the transition of electrons filling the Zn-related acceptor levels to the conduction band or to unfilled donor levels.¹⁷ This would be explained by some local inhomogeneity of the Zn and O atom densities which may give rise to empty impurity levels just above the valence band and/or filled impurity levels just below the conduction band.

The present is a hybrid density functional theory (DFT) study which provides a more accurate description of both the band gap of the two materials and the localized nature of the semicore 3d states¹⁸ of Ga and Zn, which are essential ingredients to correctly analyze solid solutions with different GaN–ZnO composition. The aim of this work is to define whether a band gap modification or impurity state introduction is the reason for the visible light absorption of the mixed GaN:ZnO solid solution.

Computational Details

Computations have been carried out with the CRYSTAL06 program.¹⁹ All-electron calculations were performed within the linear combination of atomic orbitals (LCAO) approach with the hybrid B3LYP functional,²⁰ which contains a hybrid HF and density functional exchange–correlation functional, composed of the Becke three-parameter exchange functional and the LYP²¹ correlation functional. The percentage of exact Hartree–Fock (HF) exchange in the B3LYP functional is 20%. The all-electron Gaussian-type basis set adopted is a 7311/311 basis set²² (checks with 7-311(d1)²³) for nitrogen, 86-4111(d41) for gallium,²² 8-411(d1)²⁴ for oxygen, and 8-64111(d411)²⁵ for zinc.

A 32-atom supercell obtained by an expansion matrix $2 \times 2 \times 2$ has been used for simulating the (oxy)nitride system. A

full optimization of both atomic coordinates and cell parameters has been performed.

Cut-off limits in the evaluation of Coulomb and exchange series appearing in the self-consistent field (SCF) equation for periodic systems were set to 10^{-6} for coulomb overlap tolerance, 10^{-6} for coulomb penetration tolerance, 10^{-6} for exchange overlap tolerance, 10^{-6} for exchange pseudo-overlap in the direct space, and 10^{-12} for exchange pseudo-overlap in the reciprocal space.¹⁹ The condition for the SCF convergence was set to 10^{-8} au on the total energy difference between two subsequent cycles.

The reciprocal space is sampled according to a regular sublattice with a shrinking factor (input IS) equal to 6 corresponding to 34 *k*-points in the sampling of the irreducible Brillouin zone.¹⁹

The gradients with respect to atomic coordinates and lattice parameters are evaluated analytically. The equilibrium structure is determined by using a quasi-Newton algorithm with a BFGS Hessian updating scheme.²⁶ Convergence in the geometry optimization process is tested on the root-mean-square (rms) and the absolute value of the largest component of both the gradients and nuclear displacements. For all atoms, the thresholds for the maximum and the rms forces have been set to 0.00045 and 0.00030 au, and those for the maximum and the rms atomic displacements to 0.00180 and 0.00120 au, respectively.

The densities of states (DOS) have been computed with the same *k*-point sampling as for the geometry optimizations. The Kohn–Sham eigenvalues were computed on each *k*-point of the *k*-points mesh, but only those at Γ are discussed in the paper because of the direct band gap of both GaN and ZnO. The DOS of the mixed solid solutions have been reported together with the DOS of pure GaN and ZnO in order to show how the electronic structure is modified with respect to the parent systems. The common energy zero for the different DOS corresponds to the limit of an electron at an infinite distance from the surface; that is, the zero point of orbital energy is set to the vacuum. This is done by performing a (1 × 1) slab (2D, 12 layers) calculation for pure GaN and ZnO (10-10) nonpolar surfaces. Then, the N 1s or O 1s orbital energy for one atom in the middle of the slab is used as a reference for the bulk N or O atoms in GaN and ZnO. For the mixed GaN/ZnO systems, the alignment shift is obtained as a weighted combination of the values for the pure systems, according to the number of GaN or ZnO pairs present. It should be noted that this alignment does not coincide to that resulting from photoemission measurements which also include the surface dipole contribution.

Results and Discussion

The correct description of band gap values for wide band gap semiconductors is a serious issue when discussing optical properties. Semilocal density functional theory severely underestimates band gaps of these type of materials, and therefore, any analysis based on the data derived from these methods is biased by the incorrect position of the conduction band states. Even the LDA+U or GGA+U approach does not help very much in this context, since, although the band gap value of GaN is improved (2.7 eV), that of ZnO is not as a result of the diffuse *s*-state nature of the conduction band. The on-site Coulomb interaction correction is however important for accurate description of the semicore 3d states of both Ga and Zn. One particularly attractive and relatively simple solution to both problems (description of band gap value and of localized semicore d-states) is the inclusion of a small fraction of nonlocal exchange in the Hamiltonian as in hybrid functionals. In particular, B3LYP is found to nicely reproduce group III–V semiconductor energy gaps,^{27,28} for which the result was rather

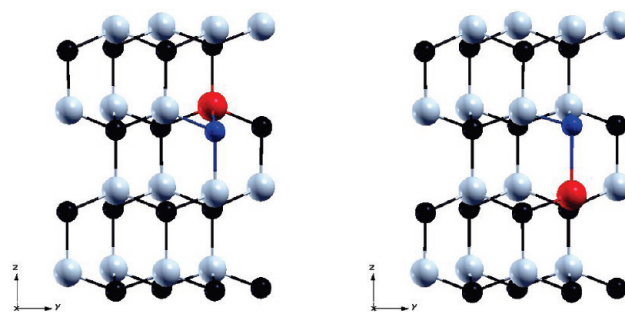


Figure 1. Configurations 1U EQUATORIAL (left) and 1U AXIAL (right) for the $x = 0.0625$ concentration of ZnO in GaN. Gallium in black, nitrogen in gray, zinc in blue, and oxygen in red.

unexpected since this hybrid functional was fitted to reproduce properties for a large set of small molecules.

With the present computational setup, we compute a 3.88 eV band gap for GaN to be compared to 3.47 eV at 0 K²⁹ (3.39 eV at 300 K)³⁰ and a 3.38 eV band gap for ZnO to be compared to 3.44 eV³¹ at 0 K (3.3 at RT).³² These values constitute a rather solid starting point for the analysis of the band gap engineering through preparation of mixed GaN:ZnO solid solutions.

The experimental studies performed on this system, in particular the X-ray diffraction (XRD) patterns, indicate a wurzite structure similar to GaN and ZnO precursors and that the obtained samples are not physical mixtures of GaN and ZnO phases but rather solid solutions. In a solid solution, one of the components behaves as the solvent while the other component (in a lower concentration) behaves as the solute. For the system under study, (Ga_{1-x}Zn_x)N_{1-x}O_x, ZnO can be considered the solute and GaN the solvent since the investigated range^{4–9} is $x = 0.05–0.42$. Note that the highest activity for overall water splitting is for $x = 0.12$.⁶ Solid solutions are expected to be homogeneous. This can be interpreted in terms of isolated ZnO units or as small ZnO clusters fully dispersed in the GaN lattice. An interesting discussion on how to simulate a random solid solution has been presented in two recent works which have been almost concomitantly published.^{15,16} Huda et al.¹⁶ have analyzed both the random alloy system (GaN)_{1-x}(ZnO)_x and the superlattices (GaN)_n(ZnO)_n. The random alloy system was simulated by introducing one pair of ZnO in the GaN supercell (or vice versa) and assuming that Zn and O tend to bond together. This is a simple approach which is however sufficiently solid for low concentrations of ZnO in GaN. More sophisticated, and more relevant for higher concentrations of the solid solution, is the approach by Jensen et al.¹⁵ who have applied the SQS (special quasirandom structures) technique to construct special small-unit-cell periodic structures which are characterized by the first few pairs and multisite correlation functions matching the corresponding perfect random solution. Also in their approach, formation of nearest neighbor Ga–N and Zn–O pairs is assumed to be energetically the most favorable. In the following, we will consider the most relevant structures which have been identified in these previous computational works and compare them with other possible configurations.

We have used a 32-atom wurzite supercell which should be sufficiently large to simulate a quasi-random system. In this supercell, 16 GaN units are present which have been substituted with an increasing number of ZnO units (*n*U with $n = 1, 2, 4, 8, 12, 15$). Also the cases in which a single Ga atom is substituted with a Zn atom or a single N atom is substituted with an O atom have been analyzed.

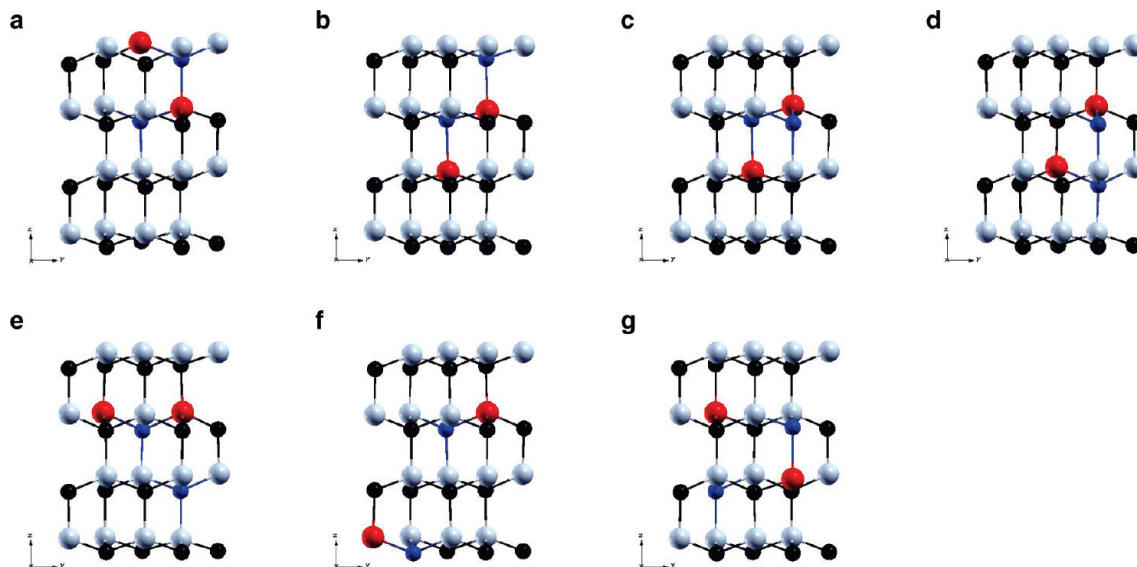


Figure 2. Configurations 2Ua–g for the $x = 0.125$ concentration of ZnO in GaN. Gallium in black, nitrogen in gray, zinc in blue, and oxygen in red.

For $x = 0.0625$ (1U case, Figure 1) we confirm (i) the assumption made in previous works that Zn and O atoms in GaN solution prefer to stick together with a stabilization energy of 0.67 eV for the most stable configuration and (ii) the result reported for other methods that the configuration with the O above the Zn (EQUATORIAL configuration, Figure 1) is more favorable than the one with the O below the Zn atom along the c -axis (AXIAL configuration, Figure 1) by about 0.24 eV. The resulting band gap for the very dilute solution based on B3LYP calculations is 3.52 eV (see Figure 5). This indicates a reduction of the band gap of GaN by about 0.35 eV (as computed with B3LYP) which however is not sufficient to account for the absorption edge in the visible region and for the reduced band gap of 2.8 eV estimated for low concentrated solid solutions (0.6–0.7 eV reduction).^{4–9} This is in contrast with results from previous theoretical studies which reported a strong reduction of the band gap value even for very low concentrations of ZnO in GaN.^{14,15} As mentioned above, their analysis was however biased by the limitations of the theoretical methods used which strongly underestimate band gap values. The electronic structure of the mixed diluted solution is characterized by a N 2p valence band edge (shifted by only +0.14 eV) with the O 2p impurity states lying at lower energies and a Zn 4s minimum conduction band (shifted by –0.2 eV), as shown in Figure 5. Note that the Zn 3d states (projected in blue) are at lower energy with respect to their position in pure ZnO.

For dilute solutions, it has been argued, on the basis of a PL and PLE study (as reported in the introduction),¹⁷ that the visible light absorption at wavelengths of 370–500 nm is not a consequence of band gap reduction but is due to impurity levels, because of local inhomogeneity of the Zn and O atom densities (corresponding to local inhomogeneity of N and Ga, respectively). We have thus investigated the possibility of having an excess of Zn (consequently of N) or O (consequently of Ga) atoms alternatively, by introducing a substitutional Zn atom in the place of Ga or a substitutional O atom in the place of N.

The Zn atom has one valence electron less than the Ga atom and therefore induces formation of an acceptor level in the nitrogen valence band. This empty state, that in a spin polarized calculation belongs to the beta set of eigenfunctions (spin down component), is actually detached from the top of the N 2p valence band and is about 2.79 eV from the bottom of the

conduction band at Γ point (see also DOS in Figure 5). Analysis of the density projected on this empty state is not achievable with the present code; however, the corresponding occupied state is confirmed to be a N 2p band state. In the hypothesis that extra electrons are present in the sample and fill this acceptor level (for example from H impurities), transitions to the conduction band would require less energy in agreement with PLE experiments. We have introduced a H atom in the system and verified that the electron from the interstitial H atom fills the acceptor level formed upon Ga substitution with Zn. The filled state is stabilized by 0.33 eV and thus is 3.12 eV below the CB minimum at Γ point (see also DOS in Figure 5). This result, given the slight overestimation of the GaN with the present computational setup, could explain the red-shift of the absorption edge of the samples presenting unbalanced concentrations of Zn with respect to O ions.

On the contrary, the O atom presents one more valence electron than the N atom, and therefore, its substitution of the N atom in GaN induces formation of a donor level which is located below the bottom of the conduction band of about 0.7 eV at Γ point. Analysis of this state indicates a strong Ga 4s character, localized on the Ga ions neighboring the O impurity. The presence of this state and of the corresponding empty level can provide an explanation for the excitations in the visible region (see Figure 5).

For higher concentrations, the analysis becomes more complicated because of a variety of possible configurations for the solute ZnO units in GaN. The two compounds of the alloy can be organized in a random system or in an ordered superlattice. The present calculations clearly show that the ordered superlattice total energy is lower than that for the random alloy system as we will see in the following.

When $x = 0.125$ (2U, Figure 2), in $(\text{Ga}_{1-x}\text{Zn}_x)\text{N}_{1-x}\text{O}_x$, corresponding to two ZnO units in the 32-atom model supercell, there are a number of possible relative arrangements of the two ZnO units. We have considered seven possible configurations: (a) the two ZnO units are in the EQUATORIAL configuration and bound one to the other in a zigzag fashion in two different layers; (b) the two ZnO units are in the AXIAL configuration on two parallel vertical lines connected through a Zn–O bond; (c) one ZnO unit is in the EQUATORIAL and the other is in the AXIAL configuration connected through a Zn–O bond;

TABLE 1: Energy Differences (in eV) Referred to the Most Stable Configuration for $x = 0.125$ Concentration (2U)^a

$x = 0.125$	ΔE (in eV)	Δa	Δc	band gap Γ
2Ue	0	+0.022	+0.030	3.48
2Ua	0.35	+0.021	+0.032	3.50
2Uf	0.63	+0.017	+0.029	3.32
2Ub	0.68	+0.026	+0.041	2.83
2Uc	0.70	+0.024	+0.037	2.95
2Ud	0.84	+0.027	+0.033	3.20
2Ug	1.12	+0.023	+0.043	3.26

^a Variations in the lattice parameters (in Å) with respect to bulk GaN. Band gap values in eV.

(d) the two ZnO units are in the EQUATORIAL configuration in two parallel layers but are not connected one to the other; (e) the two ZnO units are in the EQUATORIAL configuration in the same layer connected through a Zn–O bond; (f) the two ZnO units are in the EQUATORIAL configuration far apart in the supercell; (g) one ZnO unit is in the AXIAL configuration while the other one is splitted in nonbonded Zn and O atoms along the same c -axis direction. This last configuration has been considered because it was found by Jensen et al.¹⁵ to be the most stable one in a 16-atom supercell (twice the ZnO concentration) and by means of the PBE+U method. The present B3LYP calculations indicate the configuration 2Ue as the most stable according to the data in Table 1. The lattice parameter deformations with respect to those obtained for the fully relaxed GaN system are also reported in Table 1 ($a = 3.218$ Å and $c = 5.230$ Å).

The data on the electronic structure of the various configurations considered are rather surprising. The band gap values at Γ span a rather broad window from 3.5 to 2.8 eV. Thus, the most stable configuration 2Ue is characterized by a band gap of 3.48 eV, very close to that computed for the lower concentration ($x = 0.0625$) which again cannot explain the visible light absorption in the observed range and cannot account for the estimated 2.6–2.8 eV band gap^{4–9}. Two possible alternative explanations for the red-shift of the absorption edge are possible. As in the case of very diluted solid solutions, one

TABLE 2: Energy Differences (in eV) Referred to the Most Stable Configuration for $x = 0.25$ Concentration (4U)^a

$x = 0.25$	ΔE (in eV)	Δa	Δc	band gap Γ
4Ua	0	+0.027	+0.047	3.35
4Uc	0.19	+0.031	+0.048	3.44
4Ud	0.56	+0.040	+0.045	3.41
4Ue	0.76	+0.036	+0.055	3.24
4Ub	1.65	+0.040	+0.081	2.10

^a Variations in the lattice parameters (in Å) with respect to bulk GaN. Band gap values in eV.

can invoke the presence of impurity levels (see discussion above). Alternatively, one may suppose that configurations whose overall total electronic energy is not the lowest, that is, which from the energetic (enthalpic) point of view are not the most stable, may become more or equally favorable if one does also take into account entropic factors in random alloy systems. At the high temperatures of annealing performed on the samples (about 1100 K), it is reasonable to suppose that the entropic term is substantial in the thermodynamic analysis.

For the random alloy configurations, we compute 2.83 and 2.95 eV band gaps. Further analysis of the electronic structure (see also DOS for 2Ub in Figure 6) indicates that the bottom of the conduction band (CB) is slightly shifted toward lower energies with respect to the pure GaN system, while the top of the valence band (VB), N 2p states, is shifted toward higher energies. In particular, the highest occupied state is essentially composed by the 2p states of the N atoms directly bound to the Zn atoms. This energy enhancement is the consequence of the N 2p and Zn 3d electronic repulsion, as proved by the further upward shift of the Zn d states with respect to their position in a more diluted system. Note that only the DOS of two configurations (2Ua and 2Ub) have been reported in Figure 6 which present the largest (3.50 eV) and the lowest (2.83 eV) band gap values, respectively. In general we can note that the position of the 3d Zn states is symptomatic of the degree of repulsion with the N 2p states and thus of the band gap reduction. For example, it is interesting to compare the 2Ua

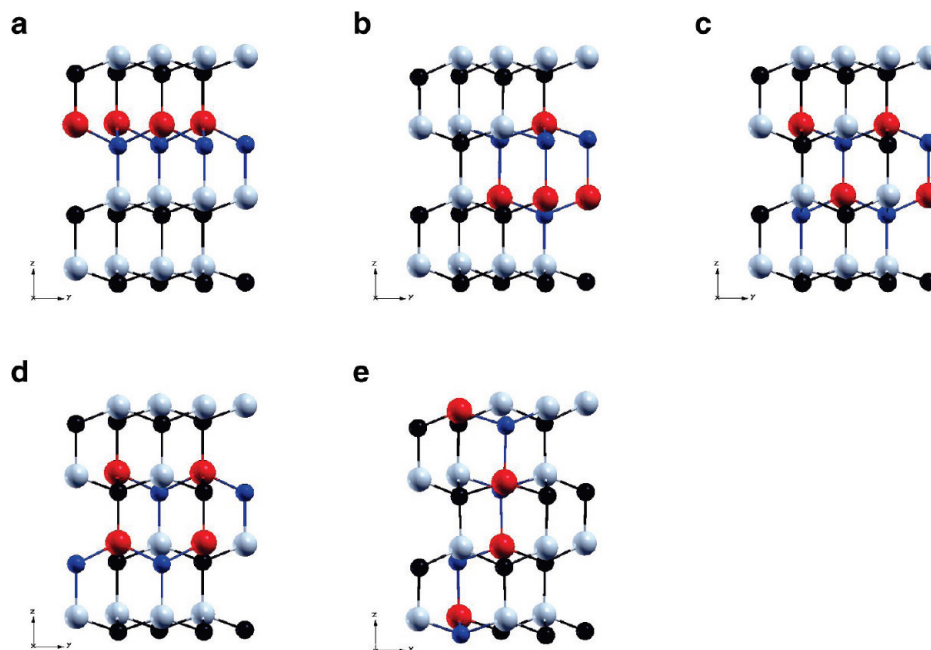


Figure 3. Configurations 4Ua–e for the $x = 0.25$ concentration of ZnO in GaN. Gallium in black, nitrogen in gray, zinc in blue, and oxygen in red.

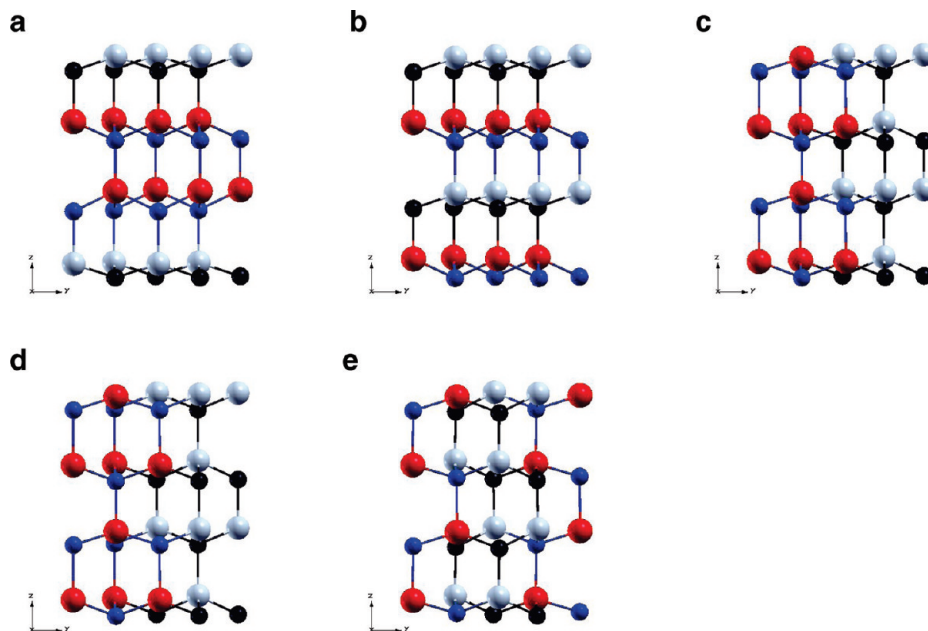


Figure 4. Configurations 8Ua–e for the $x = 0.5$ concentration of ZnO in GaN. Gallium in black, nitrogen in gray, zinc in blue, and oxygen in red.

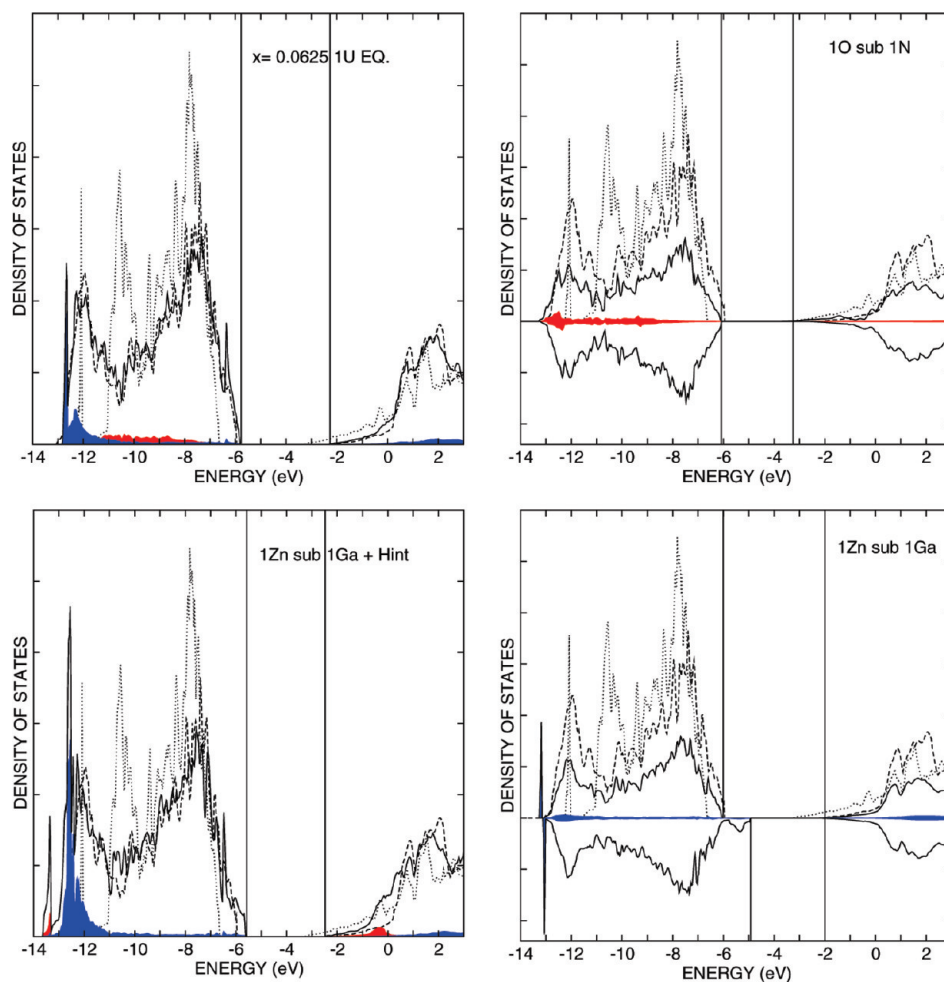


Figure 5. Density of states (DOS) for the $x = 0.0625$ concentration of ZnO in GaN (1U EQUATORIAL case, upper left panel); DOS for the 1O substitutional to 1N atom (upper right panel); DOS for 1Zn substitutional to 1Ga atom (lower right panel); and DOS for 1Zn substitutional to 1Ga atom and an additional interstitial H (lower left panel). The two panels on the right have both the up and down spin component because they are derived from spin-polarized calculation in the doublet spin state. The total DOS is the solid black line, while projected density of states (PDOS) on Zn atoms is in blue, on O atoms in red, and on H atom in brown. The dashed line represents the total DOS for GaN, and the dotted line represents the total DOS of ZnO. Vertical lines indicate the top of the VB and the bottom of the CB for the mixed system.

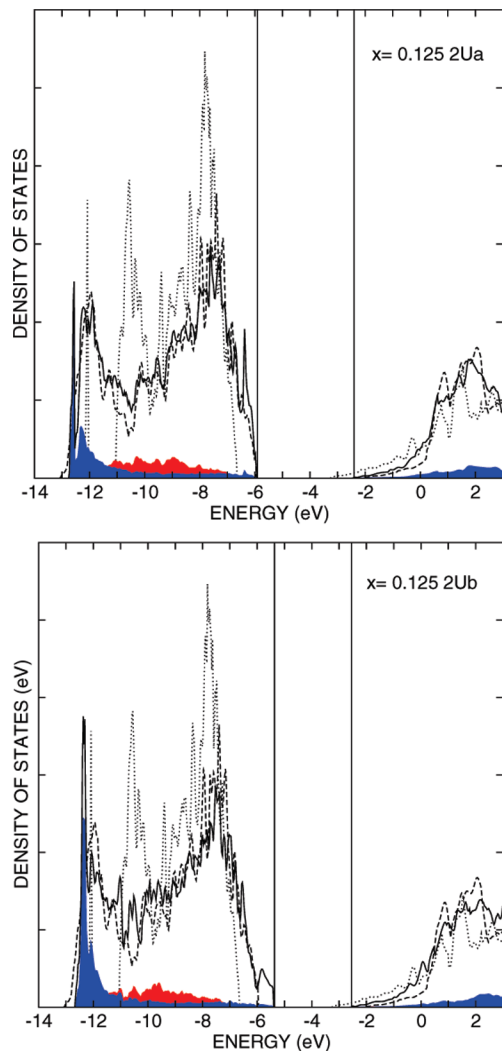


Figure 6. Density of states (DOS) for two configurations with $x = 0.12$ concentration of ZnO in GaN (2Ua, upper panel and 2Ub, lower panel). The total DOS is the solid black line, while projected density of states (PDOS) on Zn atoms is in blue and on O atoms in red. The dashed line represents the total DOS for GaN, and the dotted line represents the total DOS of ZnO. Vertical lines indicate the top of the VB and the bottom of the CB for the mixed system.

TABLE 3: Energy Differences (in eV) Referred to the Most Stable Configuration for $x = 0.5$ Concentration (8U)^a

$x = 0.5$	ΔE (in eV)	Δa	Δc	band gap Γ
8Ub	0	+0.051	+0.081	3.36
8Ua	0.56	+0.053	+0.098	3.06
8Ue	2.53	+0.071	+0.148	2.43
8Uc	2.87	+0.078	+0.124	2.03
8Ud	2.87	+0.078	+0.124	3.27

^a Variations in the lattice parameters (in Å) with respect to bulk GaN. Band gap values in eV.

and the 2Ub cases and observe that the 3d states are of course at higher energy for the 2Ub model system.

When $x = 0.25$ (4U, Figure 3), there are four ZnO units in the 32-atom supercell. We have considered five possible configurations: (a) a superlattice configuration where one layer in the (0001) plane is fully ZnO structure while the other three layers are GaN; (b) the four ZnO units are the basis of two connected tetrahedra of Zn and O atoms forming a compact ZnO structure in the GaN matrix; (c) the four ZnO units are all connected on one side of the hexagonal supercell; (d) two ZnO

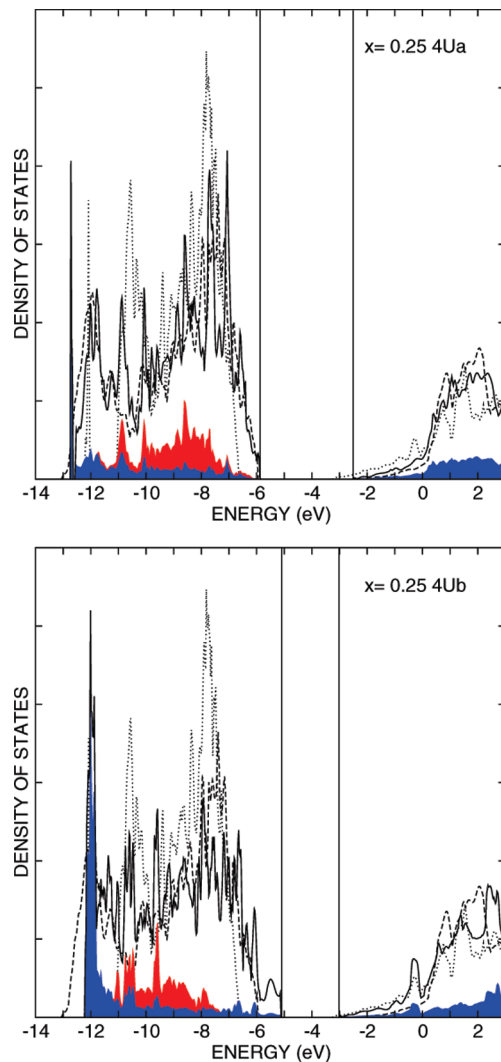


Figure 7. Density of states (DOS) for two configurations with $x = 0.25$ concentration of ZnO in GaN (4Ua, upper panel and 4Ub, lower panel). The total DOS is the solid black line, while projected density of states (PDOS) on Zn atoms is in blue and on O atoms in red. The dashed line represents the total DOS for GaN, and the dotted line represents the total DOS of ZnO. Vertical lines indicate the top of the VB and the bottom of the CB for the mixed system.

units are connected on one side of the hexagonal supercell while the other connected two units are on the other side of the supercell in another (0001) layer; (e) the four ZnO units are connected through a single ZnO in a long zigzag chain. This last configuration was found to be the most stable by Jensen et al.¹⁵ on the basis of SQS and PBU+U approaches. According to B3LYP calculations, the superlattice structure 4Ua is the most stable by 0.19 eV (Table 2). Among the more random structures, the configuration 4Uc is the most stable (Table 2). The lattice parameters deformations with respect to stoichiometric bulk GaN are also reported in Table 2.

The electronic structure is again very sensitive to the solute configuration in the solvent matrix. The band gap value in Γ for the superlattice configuration is 3.35 eV. The values for the more random alloy configurations span from 3.44 to 2.10 eV. Also for this concentration, the absorption in the visible range can be rationalized by supposing either that some nonstoichiometric Zn or O impurities are present in the samples forming impurity states in the band gap, or, more probably, that the random solutions with largely smaller band gaps become feasible because of entropic factors playing a major role when high

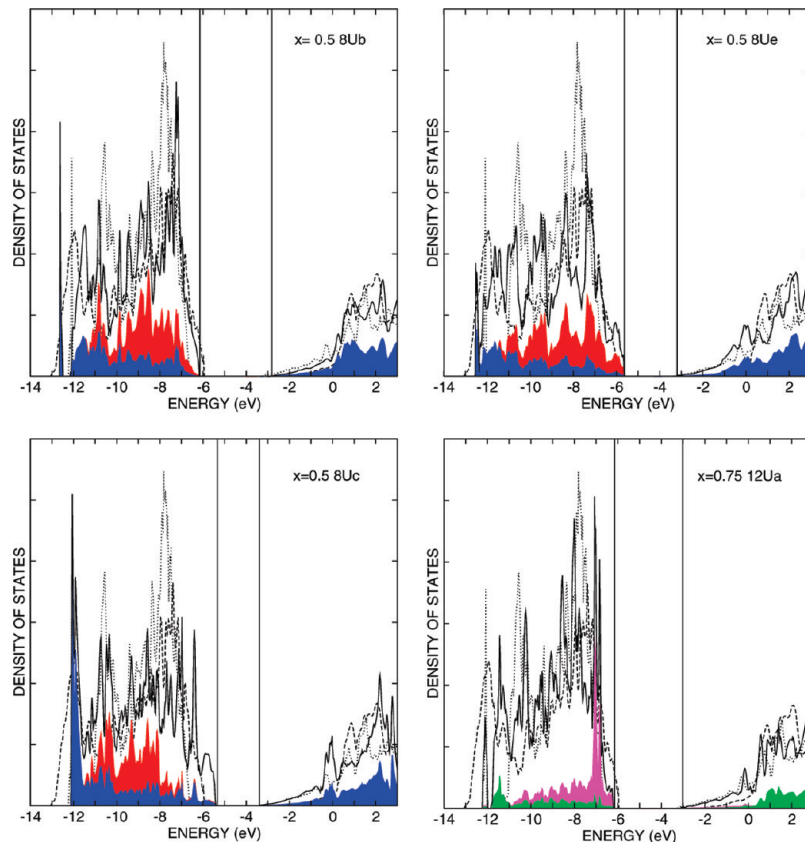


Figure 8. Density of states (DOS) for three configurations with $x = 0.5$ concentration of ZnO in GaN (8Ub, upper left panel, 8Uc, upper right panel, 8Ue, lower left panel). The total DOS is the solid black line, while projected density of states (PDOS) on Zn atoms is in blue and on O atoms is in red. Total DOS for one configuration with $x = 0.75$ concentration of ZnO in GaN (12Ua, lower right panel). The projected density of states (PDOS) on Ga atoms is in green and on N atoms in magenta. The dashed line represents the total DOS for GaN, and the dotted line represents the total DOS of ZnO. Vertical lines indicate the top of the VB and the bottom of the CB for the mixed system.

TABLE 4: Energy Differences (in eV) Referred to the Most Stable Configuration for $x = 0.75$ Concentration (12U)^a

$x = 0.75$	ΔE (in eV)	Δa	Δc	band gap Γ
12Ua	0	+0.086	+0.127	3.11
12Uc	0.50	+0.104	+0.119	3.02
12Ud	0.77	+0.115	+0.106	3.09
12Ue	1.04	+0.108	+0.134	2.77
12Ub	1.56	+0.113	+0.114	1.84

^a Variations in the lattice parameters (in Å) with respect to bulk GaN. Band gap values in eV.

temperature treatments are performed. The smallest band gap of 2.1 eV is computed for the highly unstable configuration 4Ub. The analysis of the electronic structure (see also DOS 4Ub in Figure 7) shows that the bottom of the CB is shifted to lower energies and at the same time the top of the VB is largely shifted toward higher energy. The upper VB is made up by the 2p states of the N atoms directly bound to and in the same plane as three of the four Zn atoms introduced in the supercell. The higher the Zn–N bonds in the (0001) plane, the higher the total energy and the smaller the band gap of the system. Note that only the DOS of two configurations (4Ua and 4Ub) have been reported in Figure 7 which are the most stable with large band gap values (3.35 eV) and the least stable with the smallest band gap value (2.10 eV), respectively. Again, it is worthwhile noting the different position of the Zn 3d states in the two representative model systems. For the 4Ub case with a very large band gap reduction, the 3d Zn peak is about 1 eV higher in energy than that in the 4Ua case. These correlations are very important to

show that the band gap reduction is strictly connected to the Zn and N vicinity and to their 3d–2p full states repulsion.

For $x = 0.5$ (8U, Figure 4), with the two materials equally present in the alloy, we are considering a concentration of ZnO which is slightly larger than the highest ($x = 0.42$) concentration tested in the seminal brief communication by Domen and co-workers.⁷ Five possible configurations have been investigated: (a) a superlattice structure with the eight ZnO units in two subsequent (0001) layers; (b) a superlattice structure with the eight ZnO units in two separated (0001) layers; (c) a superlattice structure with the GaN–ZnO interface on the (1100) surface; (d) a superlattice structure with the GaN–ZnO interface on the (1010) surface; (e) a random alloy with the ZnO units along zigzag chains, in a similar fashion as for configuration 4Ue for $x = 0.25$. Configuration 8Uc was found to be the most stable superlattice system in a GGA+U study by Huda et al.,¹⁶ while configuration 8Ue was found to be the most stable configuration for a random alloy by Jensen et al.¹⁵ on the basis of SQS and PBU+U approaches. B3LYP total energy indicates that the most stable configuration is 8Ub (Table 3).

The band gap value of the superlattice structures is about 3.36 eV (except for configuration 8Uc) with a 2.03 eV band gap), while that for the random alloy structure is 2.43 eV (configuration 8Ue) at Γ point. Further analysis of the electronic structure of configurations 8Uc and 8Ue shows that the band gap reduction is a consequence of the fact that the top of the VB is very similar to GaN's while the bottom of the CB is very close to the ZnO's. The top of the VB essentially composed by the N 2p states of the interface atoms is observed. Note that only the DOS of three configurations (8Ub, 8Uc, and 8Ue) have

been reported in Figure 8 which are the most stable with large band gap values (3.36 eV), the least stable with the smallest band gap value (2.03 eV), and the random alloy structure (2.43 eV), respectively. The overall electronic structure and band position is progressively less similar to pure GaN and closer to pure ZnO.

In the present work, the possibility to have a solution of GaN in ZnO has also been investigated, although the experimental photocatalyst, which has been prepared and has shown to present promising activity in the visible light spectrum, is a solution of ZnO in GaN, as described in the Introduction. However, this can be considered a computational exercise which was performed by others before with different methods.¹⁵ Two possible x values have been considered: $x = 0.75$ (12U) and $x = 0.9375$ (15U, see corresponding structure in Figure 1) for (Ga_{1-x}Zn_x)N_{1-x}O_x. The symmetrical configurations reported for $x = 0.25$ (with Zn and O atoms in the place of Ga and N, and vice versa, see corresponding structures in Figure 3) have been investigated for $x = 0.75$ (12U). The most stable configuration is the superlattice structure 12Ua while the more random structure 12Uc is only 0.50 eV higher in energy within the B3LYP approach.

The band gap value at Γ point for configuration 12Ua, the most stable, is 3.11 (see also DOS in Figure 8) and for 12Uc is 3.02 eV (Table 4). These are rather low values and make the system rather interesting. As reported before, introducing GaN in a ZnO solution can be more efficient for band gap narrowing, from a theoretical point of view, than introducing ZnO in a GaN solution.

However, this conclusion is not so general and should be confirmed experimentally. In particular, it is important to distinguish between highly concentrated or diluted solid solutions. In the case of diluted solutions, $x = 0.9375$ (15U), in the EQUATORIAL configuration for the GaN unit in the ZnO matrix, a band gap value of 2.69 eV is computed. For this concentration, however, it is more correct to talk about energy difference between N 2p defect states to the conduction band minimum edge, than of band gap narrowing. The N 2p states that lie at higher energy than the O 2p states are only slightly mixed with the valence band. These data nicely correlated with what has been found with the same method for a N-doped ZnO system.³³ The interest in the mixed system with ZnO as solute and GaN as solvent is not so large for photocatalytic purposes because, unless the concentration is very high, the valence band is essentially made up by O 2p states while the N 2p states are impurity states with a largely localized character and thus very inefficient for photoinduced hole transport.

Conclusions

The difficulty of standard density functional theory to accurately describe semiconductor band gaps is a well-known problem which becomes a basic issue when one wants to analyze the modification of the electronic structure going from the pure GaN and ZnO systems to a mixed solid solution of the two materials. For this reason, we have performed a detailed study based on the hybrid density functional B3LYP which is found to be more reliable than classical semilocal approximations for band gap prediction, as a consequence of the nonlocal Fock exchange present in the Hamiltonian.²⁷ Our results nicely reproduce band gap values of both GaN and ZnO systems. In the case of diluted solutions of ZnO in GaN, very small band gap modifications are computed and thus local inhomogeneity of Zn or O concentration must be invoked to reproduce the absorption edge red-shift as experimentally observed. For larger

concentrations, we must first note that GaN and ZnO tend to segregate in superlattice systems from the energetic point of view. However, at the temperature of annealing of the samples (1100 K), the entropic term becomes very important and therefore the possibility to have random alloy systems is the most probable. The characterization of the GaN:ZnO samples indicates that the solid state solutions exhibit single-phase diffraction patterns. Our calculations show that the random alloy distributions, enthalpically more expensive but entropically more favorable, are found to present largely reduced band gap values because of a positive shift of the N 2p states from the GaN component interfacing the ZnO fragments, because of the electronic repulsion with the 3d Zn states. Such reduction can explain the observed absorption in the visible region. On the contrary, in most cases, the superlattice systems are energetically more stable because of the lower number of interface ions but consequently present a smaller reduction of the band gap value with respect to the parent materials.

Acknowledgment. The CILEA supercomputing center is acknowledged for the computer time provided to run this project. I am grateful to G. Pacchioni and A. Selloni for their critical comments on the manuscript.

References and Notes

- (1) Kudo, A.; Miseki, Y. *Chem. Soc. Rev.* **2009**, *38*, 253.
- (2) Honda, K.; Fujishima, A. *Nature* **1972**, *238*, 37.
- (3) Kudo, A.; Kato, H.; Tsuji, I. *Chem. Lett.* **2004**, *33*, 1534.
- (4) Maeda, K.; Domen, K. *J. Phys. Chem. C* **2007**, *111*, 7851.
- (5) Maeda, K.; Takata, T.; Hara, M.; Saito, N.; Inoue, Y.; Kobayashi, H.; Domen, K. *J. Am. Chem. Soc.* **2005**, *127*, 8286.
- (6) Maeda, K.; Teramura, K.; Takata, T.; Hara, M.; Saito, N.; Toda, K.; Inoue, Y.; Kobayashi, H.; Domen, K. *J. Phys. Chem. B* **2005**, *109*, 20504.
- (7) Lu, D.; Takata, T.; Saito, N.; Inoue, Y.; Domen, K. *Nature* **2006**, *440*, 295.
- (8) Maeda, K.; Hashiguchi, H.; Masuda, H.; Abe, R.; Domen, K. *J. Phys. Chem. C* **2008**, *112*, 3447.
- (9) Maeda, K.; Teramura, K.; Domen, K. *J. Catal.* **2008**, *254*, 198.
- (10) Sakthivel, S.; Janczarek, M.; Kisch, H. *J. Phys. Chem. B* **2004**, *108*, 19384.
- (11) Watanabe, Y.; Hashimoto, K. *J. Phys. Chem. B* **2003**, *107*, 5483.
- (12) Nakamura, R.; Tanaka, T.; Nakato, Y. *J. Phys. Chem. B* **2004**, *108*, 10617.
- (13) Di Valentin, C.; Pacchioni, G.; Selloni, A.; Livraghi, S.; Giamello, E. *J. Phys. Chem. B* **2005**, *109*, 11414.
- (14) Wei, W.; Dai, Y.; Yang, K.; Guo, M.; Huang, B. *J. Phys. Chem. C* **2008**, *112*, 15915.
- (15) Jensen, L. L.; Muckerman, J. T.; Newton, M. D. *J. Phys. Chem. C* **2008**, *112*, 3439.
- (16) Huda, M. N.; Yan, Y.; Wei, S.-H.; Al-Jassim, M. M. *Phys. Rev. B* **2008**, *78*, 195204.
- (17) Hirai, T.; Maeda, K.; Yoshida, M.; Kubota, J.; Ikeda, S.; Matsumura, M.; Domen, K. *J. Phys. Chem. C* **2007**, *111*, 18853.
- (18) Di Valentin, C.; Pacchioni, G.; Onishi, H.; Kudo, A. *Chem. Phys. Lett.* **2009**, *469*, 166.
- (19) Dovesi, R.; Saunders, V. R.; Roetti, C.; Orlando, R.; Zicovich-Wilson, C. M.; Pascale, F.; Civalieri, B.; Doll, K.; Harrison, N. M.; Bush, I. J.; D'Arco, Ph.; Llunell, M. *CRYSTAL06 User's Manual*; University of Torino: Italy, 2006.
- (20) Becke, A. D. *J. Chem. Phys.* **1993**, *98*, 5648.
- (21) Lee, C.; Yang, W.; Parr, R. G. *Phys. Rev. B* **1988**, *37*, 785.
- (22) Pandey, R.; Causà, M.; Harrison, N. M.; Seel, M. *J. Phys.: Condens. Matter* **1996**, *8*, 3993.
- (23) Pandey, R.; Jaffe, J. E.; Harrison, N. M. *J. Phys. Chem. Solids* **1994**, *55*, 1357.
- (24) Noel, Y.; Zicovich-Wilson, C. M.; Civalieri, B.; D'Arco, Ph.; Dovesi, R. *Phys. Rev. B* **2001**, *65*, 014111.
- (25) Homann, T.; Hotje, U.; Binnewies, M.; Börger, A.; Becker, K. D.; Bredow, T. *Solid State Sci.* **2006**, *8*, 44.
- (26) Civalieri, B.; D'Arco, P.; Orlando, R.; Saunders, V. R.; Dovesi, R. *Chem. Phys. Lett.* **2001**, *348*, 131.
- (27) Muscat, J.; Wander, A.; Harrison, N. M. *Chem. Phys. Lett.* **2001**, *342*, 397.
- (28) Tomiæ, S.; Montanari, B.; Harrison, N. M. *Phys. E* **2008**, *40*, 2125.

(29) Bougrov, V.; Levinshtein, M. E.; Rumyantsev, S. L.; Zubrilov, A. In *Properties of Advanced Semiconductor Materials GaN, AlN, InN, BN, SiC, SiGe*; Levinshtein, M. E., Rumyantsev, S. L., Shur, M. S., Eds.; John Wiley & Sons, Inc: New York, 2001; p 1–30.

(30) Chow, T. P.; Ghezzo, M. J. SiC power devices. In *III-Nitride, SiC, and Diamond Materials for Electronic Devices*, Material Research Society Symposium Proceedings, Pittsburgh, PA; Gaskill, D. K., Brandt, C. D., Nemanich, R. J., Eds.; 1996; Vol. 423, pp 69–73.

(31) Reynolds, D. C.; Look, D. C.; Jogai, B.; Litton, C. W.; Cantwell, G.; Harsch, W. C. *Phys. Rev. B* **1999**, *60*, 2340.

(32) Özgür, Ü *J. Appl. Phys.* **2005**, *98*, 041301.

(33) Gallino, F.; Di Valentin, C.; Pacchioni, G.; Chiesa, M.; Giamello, E. *J. Mater. Chem.* **2010**, *20*, 689.

JP9112552